Hematopoietic cell-derived RELMα regulates hookworm immunity through effects on macrophages

Hashini M. Batugedara[*], **Jiang Li**[*], **Gang Chen**[*], **Dihong Lu**[†], **Jay J. Patel**[*], **Jessica C. Jang**[*], **Kelly C. Radecki**[*], **Abigail C. Burr**[*], **David D. Lo**[*], **Adler R. Dillman**[†], and **Meera G. Nair**[*]

[*]Division of Biomedical Sciences, School of Medicine, University of California Riverside, Riverside, CA

[†]Department of Nematology, University of California Riverside, Riverside, CA

Abstract

Resistin-like molecule α (RELMα) is a highly-secreted protein in type 2 (Th2) cytokine-induced inflammation including helminth infection and allergy. In infection with *Nippostronglyus brasiliensis* (*Nb*), RELMα dampens Th2 inflammatory responses. RELMα is expressed by immune cells, and by epithelial cells (EC), however, the functional impact of immune versus EC-derived RELMα is unknown. We generated bone marrow (BM) chimeras that were RELMα deficient (RELMα$^{-/-}$) in BM or non BM cells and infected them with *Nb*. Non BM RELMα$^{-/-}$ chimeras had comparable inflammatory responses and parasite burdens to RELMα$^{+/+}$ mice. In contrast, both RELMα$^{-/-}$ and BM RELMα$^{-/-}$ mice exhibited increased *Nb*-induced lung and intestinal inflammation, correlated with elevated Th2 cytokines and *Nb* killing. CD11c$^+$ lung macrophages were the dominant BM-derived source of RELMα and can mediate *Nb* killing. Therefore, we employed a macrophage-worm co-culture system to investigate whether RELMα regulates macrophage-mediated *Nb* killing. Compared to RELMα$^{+/+}$ macrophages, RELMα$^{-/-}$ macrophages exhibited increased binding to *Nb* and functionally impaired *Nb* development. Supplementation with recombinant RELMα partially reversed this phenotype. Gene expression analysis revealed that RELMα decreased cell adhesion and Fc receptor signaling pathways, which are associated with macrophage-mediated helminth killing. Collectively, these studies demonstrate that BM-derived RELMα is necessary and sufficient to dampen *Nb* immune responses, and identify that one mechanism of action of RELMα is through inhibiting macrophage recruitment and interaction with *Nb*. Our findings suggest that RELMα acts as an immune brake that provides mutually beneficial effects for the host and parasite by limiting tissue damage and delaying parasite expulsion.
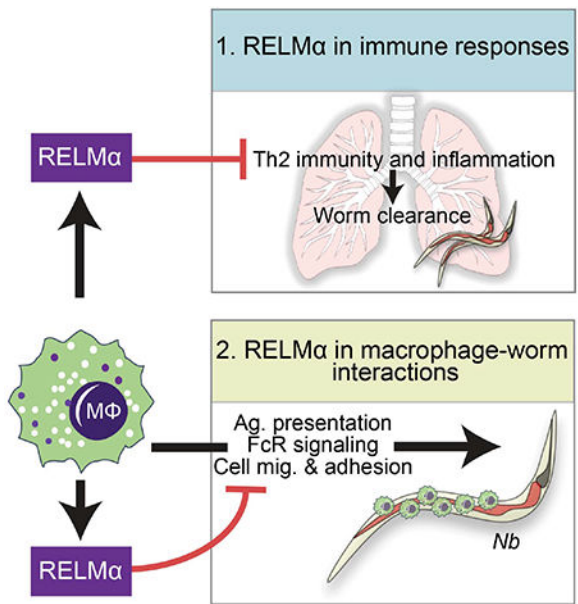
Graphical Abstract

Author Manuscript

Author Manuscript

Author Manuscript

Author Manuscript

SUMMARY:

Employing hookworm infection of RELMα$^{-/-}$ bone marrow chimeras, co-culture assays and gene expression analysis, we show that lung macrophage-derived RELMα downregulates inflammation and parasite killing.

Keywords

Macrophage; Parasitic-helminth; Inflammation; Lung; Bone marrow chimera

INTRODUCTION

Infections with parasitic worms induce a T helper type 2 (Th2) immune response that is important for controlling parasite burdens during primary infection and for immunity to subsequent secondary infections [1–4]. Additionally, Th2 immune responses have evolved to rapidly repair tissue damage caused by parasitic worms, and to restore tissue integrity and homeostasis following parasite killing [5–7]. However, excessive Th2 immune responses are detrimental to the host where they can contribute to allergic inflammatory responses and tissue fibrosis [8–10]. Therefore, Th2 immune responses must be carefully balanced for optimal anti-parasitic immunity and tissue repair while limiting excessive inflammation and fibrosis. Investigation of host factors that regulate such immune responses could have broad implications for the treatment of these pathologies. Here we investigated the contribution of Resistin-like molecule α (RELMα/Rα) to this host regulatory pathway in helminth infection.

RELMα is a host-derived protein that is highly expressed in several disease conditions including helminth infection, colitis, diabetes, allergy and asthma [11–16]. In mouse models of asthma, RELMα expression is elevated in the lung following allergen challenge, where it

was postulated to promote to airway hyperresponsiveness [11, 17, 18]. Other studies using genetic deletion of RELMα or RELMα overexpression have suggested instead a beneficial function for RELMα in limiting Th2 cytokine-induced inflammation in mouse models of asthma and mouse helminth infection [19–21]. Although protective in dampening lung inflammatory responses, RELMα paradoxically impaired optimal parasite expulsion in infection with the hookworm *Nippostrongylus brasiliensis* (*Nb*) [19, 21].

The mechanism of RELMα-induced immunoregulation has been investigated in *in vitro* activated bone marrow-(BM) derived macrophages and dendritic cells [13, 22–24]. These studies showed that RELMα expressed by alternatively activated macrophages (AAMac) dampened CD4$^+$ Th2 cell responses while RELMα derived from dendritic cells promoted CD4$^+$ IL-10 production. However, whether *in vivo* derived RELMα from these immune cells functionally impacts helminth infection-induced inflammatory response or helminth expulsion is unclear. Indeed, RELMα is also expressed by non-immune cells such as airway epithelial cells (EC), although the function of non-immune cell-derived RELMα is less well understood. In contrast to immune cells which can traffic to various sites in the body, EC cells are stationary and provide a barrier against pathogens. Nevertheless, EC contribute to host protective immunity by secreting chemokines and other proteins, such as trefoil factors, that mediate lung tissue repair following hookworm infection [25].

In this study, we investigated the functional contribution of RELMα derived from immune and non-immune cells and explored the mechanism of RELMα inhibition of helminth expulsion. Employing RELMα deficient BM chimeras, we show that immune cell-derived RELMα, and not EC-derived RELMα, downregulates the Th2 inflammatory response against hookworms and impairs clearance of worms by the host. Further, we identify CD11c$^+$F4/80$^+$ macrophages as the primary source of immune cell-derived RELMα in the lungs. We utilize CD11c$^+$ macrophage-worm co-culture assays to demonstrate that RELMα impairs macrophage-worm interaction and killing. Last, to identify potential downstream mechanisms of RELMα signaling on macrophages, we utilized Nanostring technology to measure RELMα-induced changes in expression of over 700 myeloid specific genes in purified lung macrophages. Functional enrichment pathway analysis revealed that RELMα treatment downregulated genes associated with macrophage-mediated helminth killing, such as cell adhesion and Fc receptor signaling, but upregulated genes associated with cell cycle and apoptosis and Th1 activation. Collectively, our data implicate immune cell-derived RELMα as an important regulatory factor in hookworm infection through two mechanisms: 1/ inhibiting Th2 inflammatory responses and 2/ directly acting on macrophages to impair adhesion to the worm.

MATERIALS AND METHODS

Mice

C57BL/6 and CD45.1 mice purchased from the Jackson Laboratory were bred in-house. RELMα$^{-/-}$ (*Retnla$^{-/-}$*) mice were generated and genotyped as previously described [19]. Mice were age matched (6 to 14 weeks old), gender matched, and housed five per cage under an ambient temperature with a 12 hr light/12 hr dark cycle. All protocols for animal use and euthanasia were approved by the University of California Riverside Institutional

Animal Care and Use Committee (protocols A-20150028B and A-20150027E) and were in accordance with National Institutes of Health guidelines, the Animal Welfare Act, and Public Health Service Policy on Humane Care and Use of Laboratory Animals.

Bone marrow (BM) transfer

C57BL/6 (CD45.2), CD45.1 and RELMα$^{-/-}$ CD45.2 mice were used in BM chimera generation. Age and sex-matched animals were used as recipients of BM isolated from wild-type (WT) or RELMα$^{-/-}$ mice. Recipients were sub lethally irradiated twice with 600 rad and reconstituted with 3×10^6 total BM cells administered via retroorbital injection. Donor chimerism was evaluated 8 weeks later via flow cytometry using blood stained with allotype-specific antibodies that recognized CD45.1 or CD45.2 (eBioscience). Mice that showed <75% donor chimerism were excluded from further experimental analysis.

Infection

Nippostrongylus brasiliensis (Nb) hookworms were obtained from the laboratory of Graham Le Gros (Malaghan Institute, New Zealand). *Nb* life cycle was maintained in Sprague-Dawley rats purchased from Harlan Laboratories. Mice were injected subcutaneously with 500 *Nb* infectious third-stage larvae (L3) and sacrificed at days 3, 7 or 9 post-infection. The number of parasite eggs in the feces of infected mice were counted using a McMaster counting chamber and saturated salt solution on days 6–9 following infection. To quantify the number of adult worms within the small intestine, the small intestines of infected mice were cut longitudinally and incubated in phosphate buffered saline (PBS) at 37°C for 2 hr to allow worms to migrate out of the tissue. The number of worms in the intestines were then manually quantified. To generate *Nb* immune mice, mice were allowed to clear *Nb* infection and re-infected with 500 L3 at 21 days post primary infection. Immune mice were sacrificed at day 4 post-secondary infection.

Sample collection, processing, flow cytometry and cell sorting

Bronchoalveolar lavage (BAL) fluid and cells were recovered through washing twice with 800 ul of ice-cold 1× PBS. Cells were recovered by centrifugation and leukocytes were enumerated by manual counting using a hemocytometer. For flow cytometry, BAL cells were blocked with 0.6 g rat IgG and 0.6 g anti-CD 16/32 (2.4G2) and stained for 25 min with antibodies for SiglecF (E50-2440), Ly6G (1A8), MHCII (M5/114.15.2) (all from BD Biosciences); F4/80 (BM8), Ly6C (HK1.4), CD11b (M1/70), CD11c (N418), CD45.1 (A20) and CD45.2 (104) (all from eBioscience, Affymetrix). Cells were then washed and analyzed on an LSRII instrument (BD Bioscience), followed by data analysis using FlowJo v10 (Tree Star Inc.). Florescent activated cell sorting (FACS) was conducted on Moflo Astrios instrument (BD Bioscience). Cell populations were identified as follows; alveolar macrophages (CD11c$^+$F4/80$^+$), dendritic cells (CD11c^{hi}MHCII^{hi}), eosinophils (CD11c$^-$SiglecF$^+$), monocytes (CD11b$^+$Ly6C$^+$) and neutrophils (CD11b$^+$Ly6G).

Real Time Polymerase Chain Reaction (RT-PCR)

RNA from lung tissue was extracted with TRIzol (Sigma), and RNA from cells was extracted by using the Aurum total RNA minikit (Bio-rad). iScript reverse transcriptase was

used for cDNA synthesis (Bio-Rad). RT-PCR was performed with the Bio-Rad CFX Connect system using Bio-Rad CFX Manager 3.1 software. *Retnla* and glyceraldehyde 3-phosphate dehydrogenase (GAPDH) primers were purchased from Qiagen.

Cytokine Quantification

For sandwich enzyme-linked immunosorbent assay (ELISA), Greiner 96-well medium bind plates were coated with primary antibody to cytokines (RELMα, Peprotech; IL-13 and IL-4, eBioscience) overnight at room temperature. Plates were blocked with 5% newborn calf serum in 1× PBS for 1 hr at 37°C. Sera or tissue homogenates were added at various dilutions and incubated at room temperature for 2 hr. Cytokines were detected by applying biotinylated antibodies (RELMα, Peprotech; IL-13 and IL-4, eBioscience) for 1 hr at 37°C followed by incubation with streptavidin-peroxidase (Jackson Immunobiology) for 1 hr at room temperature. Substrate TMB (BD Bioscience) was added followed by addition of 2N H_2SO_4 as a substrate stop, and the optical density was captured at 450 nm. Samples were compared to a serial-fold dilution of recombinant cytokine.

Histology

Lungs were inflated with 1 ml 1 part 4% paraformaldehyde (PFA)/30% sucrose and 2 parts OCT embedding medium (Fisher Scientific) and stored overnight in 4% PFA/30% sucrose at 4°C. 1 cm of the proximal jejunum were fixed in 4% PFA overnight at 4°C. Lungs and intestines were blocked in OCT and sectioned at 12 μm. For immunofluorescence staining, sections were incubated with rabbit anti-mRELMα (1:400, Peprotech), biotinylated *griffonia simplicifolia* lectin (L400, Vector Laboratories), CC10 (1:400, Santa Cruz Biotechnology), F4/80 (1:400, eBioscience) overnight at 4°C. Sections were incubated with appropriate fluorochrome-conjugated secondary antibodies for 2 hr at room temperature and counterstained with DAPI. For pathology, lung sections were stained with hematoxylin and eosin. Sections were visualized under a DM5500B microscope (Leica).

Nippostrongylus-lung cell co-culture

Lung tissue of naive or immune WT or RELMα$^{-/-}$ mice were cut finely, incubated in 30 μg/mL DNAse (Sigma) and 1 mg/mL collagenase (Roche) for 25 min in a 37°C shaking incubator and passed through a 70 μm cell strainer to generate single cell suspensions. Cells were washed with Dulbecco's modified Eagle's medium supplemented with 10% fetal bovine serum, 1% L-glutamine, and 1% penicillin-streptomycin (all from Gibco). Red blood cells were lysed by using ammonium chloride-potassium buffer (Gibco). CD11c positive and negative populations were obtained using CD11c positive selection microbeads (Miltenyi). CD11c positive or negative cell fractions were incubated with 50-100 *Nb* L3 that were ex-sheathed with 0.25% NaOCl (Fisher Scientific) and washed in 400 μg/ml neomycin (Fisher Scientific) and 400 U/ml penicillin-streptomycin (Gibco). Where indicated, CD11c$^+$ RELMα$^{-/-}$ cell co-cultures were supplemented with 100 ng/ml recombinant RELMα protein. All treatments were supplemented with immune serum from secondary infected RELMα$^{-/-}$ *Nb*-infected mice and incubated at 37°C 5% CO_2. Co-cultures seeded with 0.2×10^6 cells were analyzed for cell adherence to worms and worm motility. Co-cultures seeded at 1×10^6 cells were analyzed for RELMα levels in culture supernatant and worm ATP assays. Supernatants were collected and frozen at −20°C for downstream analyses. Cell

adherence to worms was measured with bright field images of 5 fields of view in each triplicate well of the co-culture assay. The number of cells attached per worm were manually quantified. Worm motility was measured by collecting 15 second videos of 5 fields of view of each well of each treatment. Motility was assessed with custom-made Fiji macros as previously described [26]. For worm measurements, larvae from co-culture assays or *Nb*-infected mouse lungs were placed on a thin layer of 2% agarose pad and covered by a coverslip. Images of worms were taken using a camera (Canon EOS T5i) attached to a bright field microscope (Leica DM2500). Worm measurements were done by tracing worm length and width in bright field images. Worm length was determined by tracing the worm lengthwise long the central line. Worm width was measured by tracing the widest region of the midsection.

Adenosine triphosphate (ATP) assay

At the end of the co-culture assay, cells adhered to worms were removed by lysing with water. Larvae from each treatment were individually picked in $1\times$ PBS, mixed with CellTiter-Glo 2.0 luminescent reagent (Promega) and homogenized using a bead beater at $4°C$ for 5 min. The homogenates were centrifuged at $1,000 \times g$ for 2 min. Supernatants were transferred to a black 96-well clear-bottom plate and luminescence was recorded by using a Glomax Multi detection system (Promega). An ATP standard curve was generated by using ATP disodium salt (Sigma).

Scanning electron microscopy (SEM)

At day 7 of the co-culture assay, worms from each treatment were washed in $1\times$ PBS and fixed in 2.5% glutaraldehyde (Fisher Scientific) for 1 hr on ice. Samples were washed 3-times in $1\times$ PBS and fixed in 1% osmium (Fisher Scientific) at room temperature in the dark for 1 hr. Samples were washed 3-times in $1\times$ PBS and dehydrated in an ethanol gradient; 25% ethanol for 10 min, 50% ethanol for 10 min, 75% ethanol for 10 min and stored in 100% ethanol at $4°C$ until imaging. Samples were air dried overnight at room temperature and sputter coated in platinum and palladium. Samples were imaged using the XL30 scanning electron microscope.

Gene expression analysis by Nanostring

CD11c$^+$ macrophages/dendritic cells were sorted from D9 *Nb* infected RELMα$^{-/-}$ mouse lungs using the Moflo Astrios sorter (Beckman). 8×10^4 sorted RELMα$^{-/-}$ CD11c$^+$ cells were plated overnight in media with 10% fetal bovine (FBS), then serum-starved for 2hr in 1% FBS media. Cells were then stimulated for 4hr with control PBS or recombinant RELMα (200 ng) (n=3 per group). Cell lysates equivalent to 5×10^3 cells were prepared according to manufacturer's instructions and analyzed with Myeloid Innate Immunity v2 panel (Nanostring). Gene expression analysis was conducted using the Advanced Analysis Nanostring software. The Nanostring Advanced Analysis algorithm generated biological pathway scores by using normalized expression and extracting pathway-level information from a group of genes using the first principal component (PC) of their expression data [27]. Data for each pathway were scaled across samples before taking the first PC by dividing each gene's log2 expression values by the greater of either their standard deviation or 0.05. Pathway scores for PBS *vs.* RELMα treatments were combined from two independent

experiments and tested for statistical significance for a total of n=6 per group. Pathway scores are represented as the difference in pathway score between the two treatments and heatmaps of gene expression. Gene expression ratios (mRNA counts of RELMα/PBS) of two independent experiments were separately calculated by the Nanostring analysis software. Of the total 754 genes, differentially expressed genes (DEG) that reached p<0.06 were investigated for putative functions in published studies or according to biology pathways (NanoString nCounter Advanced Analysis https://www.nanostring.com/products/analysis-software/advanced-analysis and KEGG Pathway https://www.genome.jp/kegg/pathway.html.

Statistical analysis

All statistics were analyzed by Graphpad Prism software. Where appropriate student's t-test (for normal distribution data), Mann-Whitney nonparametric test (for asymmetric distribution data), two-way ANOVA (for analysis of more than one experiment). *, p 0.05; **, p 0.01; ***, p 0.0001.

RESULTS

Nb infection induces RELMα expression in EC and alveolar macrophages.

RELMα exhibits a remarkably diverse expression pattern and is expressed by immune and non-immune cells in a variety of Th2 inflammatory diseases, including helminth infection and airway allergic inflammation. We and others previously showed that RELMα dampens *in vivo* Th2 immune responses to helminths, and that macrophage and dendritic cell-derived RELMα regulates CD4$^+$T cell cytokine expression [13, 19, 21]. However, the contribution of RELMα derived from immune and non-immune cells *in vivo* following *Nb*-infection has not been evaluated. We examined cell-specific RELMα expression in WT C57BL/6 mice, subcutaneously injected with 500 *Nb* L3 (or control 1× PBS) and sacrificed at day 7 post-infection when RELMα protein levels in the infected tissues are highest [19, 28]. In accordance with previous studies, both the lung and small intestine, which are colonized by *Nb*, had significantly increased *Nb*-induced RELMα, however, RELMα mRNA levels were over 400-fold higher in the lung (Figure 1A). RELMα immunofluorescent (IF) staining of the lung and small intestine (Figure 1B) revealed that RELMα was expressed in the EC lining the airway (green arrow) and in lung parenchymal cells (white arrow). In the small intestine, histological assessment of RELMα staining suggested that RELMα was expressed by goblet cells in the basal crypts (green arrow) and by circulating leukocytes in the submucosa (white arrow). Although RELMα expression in non-immune airway EC and intestinal goblet cells was possible to visualize according to cell morphology, identifying the specific immune cells that express RELMα by IF staining was not possible. Instead, we performed cell sorting on dissociated lung tissue of *Nb*-infected mice, where RELMα expression is highest, followed by real time (RT)-PCR analysis of RELMα mRNA levels, normalized to a housekeeping gene. Purity of sorted cells was analyzed by flow cytometry and hematoxylin and eosin (H&E)-stained cytospins, revealing >90% purity (Figure 1C). CD11c$^+$F4/80$^+$ alveolar macrophages were the major immune cellular source of RELMα in the lung followed by CD11c$^+$MHCII$^+$ dendritic cells and CD11c$^-$SiglecF$^+$ eosinophils, whereas Ly6C$^+$ monocytes and Ly6G$^+$ neutrophils produce little to no RELMα (Figure 1D).

Together these studies reveal that *Nb* infection induces RELMα expression by lung and intestinal EC and by immune cells, specifically macrophages. To date, the contribution of each of these cellular sources of RELMα to the outcome of *Nb* infection has not been explored.

Generation of RELMα$^{-/-}$ BM chimeras to determine the contribution of BM and non BM-derived RELMα in *Nb* infection.

Given the lack of available cell-specific RELMα$^{-/-}$ mice, we took advantage of BM chimera technology to delineate the role of non-immune and immune cell-derived RELMα in *Nb* immune responses. Recipient mice were irradiated to deplete BM, followed by retroorbital transfer of donor BM. Successful reconstitution was confirmed 8 weeks later by flow cytometric analysis of the peripheral blood for expression of the congenic markers CD45.1 and CD45.2 (Figure 2A). Specific analysis of alveolar macrophages in the lung revealed greater than 96% reconstitution (Figure 2B). BM chimeric mice were infected with *Nb*, and sacrificed at day 9, followed by examination of RELMα expression. Lung IF staining revealed RELMα co-stained with macrophage-binding lectin, *Griffonia simplicifolia* lectin (GSL) in WT and non BM RELMα$^{-/-}$ mice but not BM RELMα$^{-/-}$ or RELMα$^{-/-}$ mice, validating that BM-specific RELMα deletion abrogated macrophage expression of RELMα (Figure 2C). Conversely, RELMα co-stained with airway EC marker CC10 in WT and BM RELMα$^{-/-}$ mice, but was abrogated when recipient mice were RELMα$^{-/-}$ (Figure 2D). Similarly, we examined RELMα expression in the *Nb*-infected small intestine (Figure 2E). All chimeras except RELMα$^{-/-}$ mice had RELMα$^+$ cells (red), but only WT and non BM RELMα$^{-/-}$ intestinal tissue sections had co-expression of RELMα with F4/80$^+$ macrophages (green).

We next evaluated if deletion of RELMα specifically in the BM or the non-hematopoietic cell compartment affected local or systemic RELMα protein levels. Bronchoalveolar lavage (BAL) fluid RELMα was increased in *Nb*-infected WT mice compared to naïve WT mice (Figure 2F). However, RELMα deletion in the BM (BM RELMα$^{-/-}$) did not affect BAL fluid RELMα levels, suggesting that BM cells contribute little to no RELMα in the airways. In contrast, when RELMα was deleted in airway EC (non BM RELMα$^{-/-}$), BAL fluid RELMα was significantly reduced to levels observed in naïve mice. We observed the opposite phenotype for systemic RELMα expression (Figure 2G), where BM-specific RELMα deletion significantly abrogated *Nb*-induced circulating RELMα, while non BM RELMα$^{-/-}$ mice still exhibited elevated serum RELMα levels. Together, these data delineate the contribution of immune and non-immune cell-derived RELMα in *Nb* infection, and show that RELMα in the airways is derived uniquely by non-immune cells, while immune cells are the main source of systemic RELMα in the serum. Nonetheless, the functional impact of local versus systemic RELMα in *Nb* immune responses is unknown.

BM-derived RELMα regulates *Nb* infection-induced tissue inflammation, Th2 immune responses and parasite expulsion.

To elucidate the role of BM and non BM RELMα in *Nb*-induced lung and intestinal inflammation, histological examination of lung and intestinal tissue sections from infected BM chimeric mice was performed. RELMα$^{-/-}$ and BM RELMα$^{-/-}$ mice exhibited the most

severe lung alveolar destruction (green arrow) and intestinal immune cell infiltration in the submucosa (blue arrow) (Figure 3A). In contrast, non BM RELMα$^{-/-}$ had comparable tissue inflammatory responses to WT mice, suggesting that BM-derived RELMα critically protects from *Nb*-induced tissue damage and inflammation, while non BM-derived RELMα is dispensable. Flow cytometric analysis of the BAL cells revealed that there were no significant differences in immune cell populations, however, RELMα$^{-/-}$ and BM RELMα$^{-/-}$ mice exhibited a trend towards increased Th2 inflammation including elevated eosinophils and macrophages compared to WT and non BM RELMα$^{-/-}$ mice (Figure 3B). Similarly, serum IL-13 levels and BAL fluid IL-4 levels quantified by enzyme linked immunosorbent assay (ELISA) revealed that RELMα$^{-/-}$ and BM RELMα$^{-/-}$ mice had elevated levels of these Th2 cytokines (Figure 3C).

We next determined if the increased infection-induced inflammatory responses functionally impacted *Nb* burdens (Figure 3D). RELMα$^{-/-}$ and BM RELMα$^{-/-}$ mice had significantly reduced intestinal worm and fecal egg burdens, while there were no differences between WT and non BM RELMα$^{-/-}$ mice. Therefore, although RELMα is highly expressed by non BM-derived airway EC and BM-derived immune cells, RELMα from immune cells is necessary and sufficient to downregulate *Nb* immune responses, while non BM-derived RELMα has no obvious effect on *Nb* infection. Functionally, BM-derived RELMα is host-protective by limiting tissue damage and inflammation, but also leads to higher parasite burdens likely due to impaired Th2 cytokine-mediated mechanisms of *Nb* killing.

RELMα$^{-/-}$ CD11c^{+} lung macrophages have enhanced ability to bind and impair *Nb* fitness.

Previous studies using a *Nb* vaccination model have shown that alternatively activated macrophages from the lung interact with and mediate *Nb* killing [29]. Together with our findings that RELMα deficiency specifically in immune cells enhanced *Nb* killing, we hypothesized that RELMα$^{-/-}$ macrophages would exhibit enhanced ability to kill *Nb*. We therefore investigated whether RELMα affected lung macrophage interaction and killing of *Nb* L3 in an *in vitro Nb*-lung cell co-culture assay, modified from the *Nb* vaccination studies (Figure 4A). WT and RELMα$^{-/-}$ mice were infected with *Nb* for 21 days, followed by secondary *Nb* challenge to enhance alternatively activated macrophage responses. Four days following re-infection, lungs were recovered for isolation of lung macrophages. Lung alveolar macrophages express CD11c therefore we performed CD11c enrichment by magnetic bead purification. Although lung dendritic cells also express CD11c, the percentage of lung dendritic cells (CD11c^{+}MFC2^{hi}, 20%) is lower than lung macrophages (CD11c^{+}F4/80^{+}, 60%). We first examined RELMα secretion by CD11c positive and negative fraction in response to co-culture with live *Nb* L3 (Figure 4B). Co-culture with *Nb* L3 led to increased RELMα secretion especially in the CD11c^{+} fraction. These results are consistent with the real-time PCR results of sort-purified lung cells, and confirm that CD11c^{+} macrophages express more RELMα than other immune cell-types such as eosinophils, which have been previously reported to express high RELMα levels.

We next examined CD11c^{+} lung macrophage interaction with *Nb* L3 over the course of 7 days (Figure 4C). There was equivalent cell adherence to the *Nb* at day 1 post co-culture, however, we observed that RELMα$^{-/-}$ CD11c^{+} cells exhibited increased adherence to

worms compared to WT cells starting at day 3 post co-culture, suggesting that RELMα inhibited the ability of CD11c^{+} cells to bind to *Nb*. To determine if cell adherence functionally affected *Nb*, we measured *Nb* motility in the co-culture using videos. Compared to *Nb* incubated with WT macrophages, *Nb* incubated with RELMα^{−/−} macrophages had significantly decreased motility (Figure 4D). At the end of the *in vitro* co-culture, we recovered *Nb* L3 and measured worm adenosine triphosphate (ATP) levels as a measure of worm viability (Figure 4E). There was a significant decrease in *Nb* ATP levels from RELMα^{−/−} macrophage cultures compared to WT macrophage cultures. Together, these data suggest that RELMα inhibits macrophage adherence to *Nb*, and subsequent functional effects decrease *Nb* viability.

It is possible that the enhanced phenotype of RELMα^{−/−} lung macrophages is indirect as a consequence of the elevated *in vivo* Th2 cytokine response, which would promote alternatively activated macrophage activation. Alternatively, since WT macrophages secrete RELMα *in vitro* in response to co-culture with *Nb* L3, RELMα in the supernatant may directly regulate macrophage-*Nb* interaction. To delineate direct versus indirect effects of RELMα, we supplemented RELMα^{−/−} macrophage cultures with recombinant RELMα and examined cell adherence to *Nb* and subsequent effects on *Nb* fitness. The addition of RELMα to RELMα^{−/−} macrophages partially decreased cell adherence, resulting in an intermediate phenotype between RELMα^{−/−} and WT macrophages (Figure 4B). In contrast, RELMα treatment of RELMα^{−/−} cultures completely restored *Nb* motility and ATP levels to those observed in *Nb* cultured with WT macrophages (Figure 4D-E). Together these results suggest that RELMα acts both directly on lung macrophages to suppress interaction with *Nb*, and indirectly, through other cell-types and cytokines to regulate macrophage activation.

We also examined *Nb* co-culture with CD11c^{+} cells from naïve (unvaccinated) WT or RELMα^{−/−}mice in comparison to co-culture with immune (vaccinated) CD11c^{+} mice (above). Naïve WT CD11c^{+} cells cultured with *Nb* produced significantly less RELMα than immune CD11c^{+} cells at days 3, 5 and 7 post co-culture (Figure 4F). Examination of cell adherence to Nb revealed that both naïve WT and RELMα^{−/−} cells exhibited minimal binding (Figure 4G). This was in contrast to immune cells, where RELMα^{−/−} CD11c^{+} cells adhered the most, consistent with previous findings (see Figure 4C). Finally, immune RELMα^{−/−} CD11c^{+} cells were significantly better able to impair *Nb* motility than WT CD11c^{+} cells (Figure 4H). However, no significant difference was found in unvaccinated WT or RELMα^{−/−} CD11c^{+} cells in their ability to reduce *Nb* motility. These results suggest that RELMα production and worm damage by CD11c^{+} cells require signals from the infection milieu *in vivo*.

To more closely examine the functional impact of RELMα^{−/−} cell interaction with *Nb* worms, we recovered *Nb* L3 from *in vitro* co-culture with WT or RELMα^{−/−} lung cells and measured worm size. *Nb* incubated with RELMα^{−/−} cells were shorter in length and significantly smaller in width compared to *Nb* incubated with WT cells (Figure 5A). To visualize macrophage-*Nb* interaction, we performed scanning electron microscopic (SEM) imaging of *Nb* L3 following co-culture with WT or RELMα^{−/−} macrophages (Figure 5B). SEM images revealed close interaction and adherence of both WT and RELMα^{−/−} macrophages to *Nb* L3. However, WT macrophages were rounder, and the area of focal

adhesion to the worm was small and distinct. In contrast, the focal contact point of RELMα$^{-/-}$ macrophages appeared larger in area, resulting in flatter macrophages for a more expansive contact with the worm on a per cell basis. We investigated the physiological relevance of the *in vitro* effects of RELMα$^{-/-}$ cells on *Nb* growth in *in vivo Nb* infection. WT and RELMα$^{-/-}$ mice were infected with *Nb* and sacrificed at day 3, followed by recovery of *Nb* larvae from the lungs. Although numbers of worms recovered from WT mice *vs* RELMα$^{-/-}$ mice were equivalent (Figure 5C), *Nb* recovered from RELMα$^{-/-}$ lungs were shorter in length and significantly smaller in width compared to *Nb* recovered from WT lungs (Figure 5D). While there are important differences in timing between the *in vitro* (7 days) and *in vivo* (3 days), these data both indicate that *Nb*-induced macrophages differentiated in a RELMα deficient environment exhibit an enhanced activation phenotype. We show that RELMα directly inhibits macrophage-*Nb* interaction leading to impaired *Nb* killing. Since RELMα is predominantly expressed by macrophages, these data suggest that RELMα is secreted as an inhibitory cytokine that acts back on macrophages and other cell-types to dampen *Nb*-specific immune responses.

Gene expression analysis reveals that RELMα signaling in lung macrophages downregulates pathways associated with cell adhesion and Fc receptor signaling.

We previously showed that recombinant RELMα treatment of RELMα$^{-/-}$ macrophages could restore the WT macrophage phenotype, notably the reduced ability to bind to the worm and impair its motility and fitness (see Figure 4C). Therefore, we employed this controlled *in vitro* system to delineate potential downstream mechanisms by which RELMα regulates macrophage-*Nb* interaction. We utilized Nanostring technology to screen over 750 myeloid-associated genes in RELMα$^{-/-}$ CD11c^{+} lung macrophages and identify those that were differentially expressed in response to RELMα. CD11c^{+} lung macrophages were sorted from the lungs of RELMα$^{-/-}$ mice at day 9 post *Nb* infection, with ~99% purity (Figure 6A). Macrophages were rested overnight then stimulated with control PBS or recombinant RELMα for 4 hours, followed by analysis of cell lysate for 750 myeloid associated gene-encoded mRNAs. Nanostring advanced pathway analysis of RELMα *vs.* PBS-treatment revealed a number of biological pathways that were changed in response to RELMα treatment (Figure 6B). Genes associated with Th1 cytokine and chemokine signaling, and cell cycle and apoptosis were upregulated. These results may be consistent with previous studies showing that RELMα promotes chemotaxis and proliferation [30–32]. Given that RELMα downregulates Th2 cytokines [13, 21], it is likely that Th1 cytokine signaling is conversely enhanced. In addition, genes associated with TLR signaling, antigen presentation, Fc receptor signaling, and cell migration and adhesion were significantly downregulated in the RELMα treatment compared to PBS (Figure 6C and 6D). Downregulation of cell adhesion pathways is in line with our observation that RELMα treatment impairs cell adhesion to *Nb*. Further, previous studies have shown the importance of Fc receptor-mediated nematode killing [26], therefore, downregulation of these pathways by RELMα may explain the reduced ability of macrophages to bind and impair *Nb* motility and fitness.

We further analyzed the differentially expressed genes between PBS *vs.* RELMα treatments, using the cut-off value p<0.06, and categorized them according to putative functions (Table

1). Of these, RELMα downregulated 14 genes and the remaining 18 were upregulated. Interestingly, some genes associated with alternatively activated or resolving macrophages activation were downregulated, such as *Arg1*, the macrophage inhibitory factor *Mif*, the anti-inflammatory receptors *Fpr-rs5* (member of the lipoxin receptor family N-formyl peptide receptor 1), and *Trem2* [33, 34]. Of the genes that were upregulated by RELMα, we found genes associated with wound healing (*Mmp19* and *Pdgfra*), genes associated with cell survival (*Tm7sf3, Bcl2*) and genes associated with macrophage signaling and effector functions (*Rgs1*). These results show that RELMα signaling impacts various biological pathways and we have identified potential candidate genes that might be negatively regulated by RELMα to impair adhesion to the worm and killing.

DISCUSSION

Although hookworms are intestinal parasites, their development relies on their initial migration through the host lung [35]. As such, the Th2 immune response that occurs in the lung is critical for parasite clearance, especially following secondary challenge, and needs to be considered when investigating protective immunity to hookworms [36, 37]. However, hookworm-induced lung inflammation must also be closely regulated to prevent aberrant worm-induced inflammation. Th2 cytokine-activated AAMacs are critical contributors to this delicate balance between immunity and inflammation. In *Nb* infection, these cells can directly interact with and kill the worm but also are protective in resolving infection-induced lung hemorrhage and reducing neutrophil infiltration [5, 29, 38]. AAMacs also indirectly mediate *Nb* expulsion by promoting Th2 cytokine responses and inducing intestinal smooth muscle contractility [39, 40]. AAMacs secrete factors and upregulate cell surface molecules that may contribute to these functions, however, studies delineating the contribution of these specific factors to AAMac function *in vivo* are lacking. In this study, we focused on the function of RELMα, a secreted protein that is highly expressed by AAMacs in a Th2 cytokine-dependent manner [41].

By utilizing BM chimeric mice, we tested the importance of BM-derived and EC-derived RELMα for the outcome of hookworm infection and hookworm-induced inflammation. BM-derived RELMα was found to downregulate immune cell infiltration in the lungs, IL-13 and IL-4 cytokines. Consequently, mice expressing RELMα only in BM-derived cells had higher worm burdens in the intestine compared to mice expressing RELMα in ECs. Therefore, we discovered that BM or immune cell-sourced RELMα is immunomodulatory whereas EC-sourced RELMα is not. An explanation for this observed phenotype could lie in the fundamental differences between immune cells and non-immune cells. Immune cells circulate in the blood between lymph nodes and inflamed tissue but in stark contrast, ECs are stationary cells. During an infection setting, immune cells such as AAMacs have the capacity to communicate with other immune cells as well as interact with the parasite. These data are supportive of other studies showing immunoregulatory roles of AAMacs during helminth infection. While EC-derived RELMα is not immunomodulatory in *Nb* infection, high quantities of RELMα, presumably derived from EC, is observed in airways following allergen challenge. Whether EC-derived RELMα plays a more significant role in airway inflammation associated with asthma are avenues for future research.

Quantification of RELMα mRNA in sorted lung immune cells showed that alveolar macrophages were the principal source of RELMα in BM-derived cells. To further investigate the function of macrophage-derived RELMα, we performed co-culture assays of *Nb* with WT and RELMα$^{-/-}$ CD11c^{+} lung macrophages. We show that one mechanism by which RELMα impairs *Nb* killing is through impairing macrophage adherence and interaction with the worm. We employ recombinant RELMα to show that RELMα exerts its inhibitory effects directly on the worm or the macrophage. Previous studies investigating RELM protein binding of worms have shown that RELMβ but not RELMα functionally affects helminth suggesting that the effect of RELMα may be on macrophages and not on *Nb* [42, 43]. In these studies, RELMβ inhibited worm chemotaxis. Similarly, it is possible that RELMα inhibits macrophage chemotaxis to the worm. Alternatively, RELMα could regulate macrophage expression of surface integrins that mediate macrophage adherence [26, 29].

To test which potential molecules could be regulated by RELMα, we performed Nanostring gene expression analysis of PBS or rRELMα-treated RELMα$^{-/-}$ lung macrophages sorted from *Nb*-infected mice. Among the RELMα-induced upregulated pathways were chemokine signaling and Th1 activation pathways. Our previous results showed lower Th2 cytokine expression, therefore, enhanced Th1 pathways in rRELMα-treated macrophages may be consistent with RELMα regulating the balance between Th1/Th2 immune pathways. Within the chemokine pathway, RELMα upregulated *Ccl3* and *Ccl6*, while downregulating *Ccl19* and *Mif*. The differential effects of these chemokines are unclear, but may contribute to inhibiting macrophage migration to *Nb*. Consistent with our functional data showing that RELMα impaired macrophage adhesion to *Nb*, genes associated with cell adhesion were downregulated in RELMα-treated macrophages. Additionally, genes associated with Fc receptor signaling were downregulated, which may suggest RELMα-induced impairment of Fc receptor-mediated *Nb* killing [26].

Interestingly, expression of the AAMac-specific enzyme Arginase 1 was downregulated by RELMα, however, the AAMac-secreted protein Ym1 (*Chil3*) was upregulated. Arginase 1 and its downstream products have previously been implicated in causing physical damage to *Heligmosomoides polygyrus* worms *in vitro* [26], therefore is a potential candidate gene for the reduced *Nb* viability when cultured with RELMα$^{-/-}$ macrophages. Other downregulated genes included *Fpr-rs5, Fcnb* and *Amica1*. *Fpr-rs5* is a member of formyl peptide receptor 1 family, which binds anti-inflammatory lipoxins and mediates biological responses such as Ca^{2}+ mobilization, cell attachment and migration [33, 44], *Fcnb*, ficolin B, is a pattern recognition receptor that activates the complement pathway, which has been shown to mediate helminth killing [45, 46], *Amica1* encodes a JAM transmembrane adhesion molecule that mediates myeloid cell migration and adhesion [47]. Lastly, *Fgf18* is a fibroblast growth factor that induces macrophage infiltration and M2 polarization [48]. Therefore, given their known functions, *Arg1, Fpr-rs5, Fcnb, Fgf18 and Amica1* are all RELMα-downregulated candidate genes, which could contribute to macrophage migration and adherence to worms.

For the RELMα-upregulated genes, we observed the matrix metalloproteinase *Mmp19* and the platelet-derived growth factor receptor *Pdgfra.* These genes encode factors associated with tissue repair, in line with RELMα's proposed role in this process [49], therefore

RELMα induction of these *in vivo* may contribute to enhanced lung tissue repair following *Nb*-induced acute injury [50–52]. RELMα also induced genes associated with cell survival, such as the apoptosis inhibitor *Bcl2* and Tm7sf3 [53]. TM7SF3 is a seven-span transmembrane protein that protects from cellular stress and the unfolded protein response. Increased activation of this protein by RELMα may therefore promote cell survival. These findings are consistent with a previous study showing that RELMα inhibits apoptosis [11], and suggest that RELMα preserves macrophage longevity. There are currently no known membrane receptors for RELMα, and future studies could investigate if RELMα binds TM7SF3 or a protein associated with this receptor. RELMα also induced expression of *Btg2*, p53-regulated gene associated with inhibiting proliferation [54]. This is contrary to previous studies showing that RELMα induces proliferation of endothelial and smooth muscle cell lines [55, 56], however, the RELMα effects examined here were specifically in primary macrophages, which may explain these differences. Intriguingly, RELMα upregulated expression of *Rgs1*, a G-protein signaling regulator molecule, which has been demonstrated to reduce chemotaxis and dampen chemokine receptor signaling in macrophages and decrease integrin-dependent adhesion in B cells [57]. Together, our results suggest that RELMα inhibits macrophage proliferation, promotes macrophage survival and desensitizes macrophage effector functions. Of note, these gene expression changes were measured only 4 hours post RELMα stimulation and represent macrophage-specific genes that are affected by cell-extrinsic RELMα, given that RELMα$^{-/-}$ macrophages were used. Further *in vivo* studies are needed to delineate the direct and indirect effects of RELMα on macrophages compared to other cell-types. However, these gene expression analyses provide a useful foundation and candidate genes for investigation of the RELMα receptor and downstream signaling.

An interesting observation made in the co-culture assay was that *Nb* L3 cultured with WT macrophages were more motile and viable compared to *Nb* L3 alone. The improved fitness and activity of *Nb* L3 when cultured with WT cells could indicate that the worms require cues from the host for their activity and development. Studies of schistosomes have shown that the flukes require signals from host adaptive cells for their proper development [58–60]. Similarly, it is possible that the hookworms interact with and respond to host cells such as macrophages for their development. We found that *Nb* cultured with RELMα$^{-/-}$ cells are less motile and viable compared to *Nb* with WT cells or *Nb* alone. This result could be due to significantly more immune cell damage to worms in the absence of RELMα. Our work is corroborated by previously published data that highlight the importance of macrophages and not dendritic cells in maintaining immunity to helminths [39]. However, in this study, macrophages were identified as CD11b$^+$ cells and dendritic cells were identified as CD11c$^+$ cells. In the *Nb*-infected lung, we found that macrophages co-express CD11c$^+$and CD11b$^+$. One caveat of our methodology is that by purifying CD11c$^+$ cells, we select for CD11c^{mid} lung macrophages and CD11c^{hi} dendritic cells. However, we find that alveolar macrophages are in higher frequency than dendritic cells in the lung and are the dominant cellular source of RELMα.

Given the results of the co-culture assay, we postulated that *Nb* isolated from RELMα$^{-/-}$ lungs would have decreased fitness compared to WT mice. Length and width measurements of *Nb* confirmed this as worms from RELMα$^{-/-}$ mouse lungs were smaller in size. These

data highlight the significance of the lung immune response against the worm in weakening the parasite before it reaches the gut. We and others show that fewer adult *Nb* are recovered from the intestines of RELMα$^{-/-}$ mice compared to WT mice [19, 21]. A recent publication was the first to show that *Nb* L3 feed on host red blood cells when in the lung and suggested that disrupting this feeding would lead to developmental arrest of the worm. Given the level of obstruction we see in co-culture assays where RELMα$^{-/-}$ cells bind to and paralyze *Nb*, it is a possibility, that these L3s are then unable to feed and therefore suffer growth arrest [61]. This is in line with our *ex vivo* observation that L4 recovered from RELMα$^{-/-}$ mice seem developmentally impaired compared to those isolated from WT mice. Our data suggests that macrophages in the absence of RELMα damage the worm or prevent worm feeding leading to a functional impact on worm fitness and fecundity in the intestine.

In addition to high expression in the lung by hematopoietic and non-hematopoietic, RELMα derived from hematopoietic cells is also significantly increased in the blood of *Nb*-infected mice, and may modulate circulating immune cell function. Previous studies have shown that helminth infection-induced AAMacs can differentiate in the tissue, but also arise from circulating blood monocytes [62]. In addition to the regulatory effects of RELMα on the macrophages in the lung, it is also possible that RELMα may exert regulatory effects on blood monocyte-derived AAMacs that then infiltrate the infected lung and small intestine with potential functional consequences on worm killing or tissue inflammation. Indeed, we observed increased submucosal intestinal inflammation in the BM RELMα$^{-/-}$ and RELMα $^{-/-}$ mice, suggesting a regulatory role for RELMα in the intestine. The tissue-specific localization of macrophages, and the life cycle stage of the worm, may however determine their direct or indirect effects on the worm. *Nb* L3 and L4 are present in the blood and lung respectively, therefore are more likely to interact with macrophages. In contrast *Nb* adults reside in the intestinal lumen, and expulsion is dependent on several non immune cells such as epithelial and smooth muscle cells that are nevertheless instructed by immune cells such as macrophages. Comparing RELMα's functional effects on blood macrophages or intestinal macrophages *vs.* lung macrophages could provide a more comprehensive understanding of the function of this pleiotropic molecule at different *Nb* life cycle stages.

In conclusion, our studies utilize BM chimeras and macrophage-worm co-culture assays to show that RELMα derived from macrophages downregulates *Nb*-induced inflammatory responses and subsequent *Nb* clearance partly by direct inhibition of macrophage-worm interactions. Macrophage-derived RELMα is therefore an immunomodulatory molecule that protects the host from an uncontrolled Th2 inflammatory immune response at the cost of killing parasitic worms. Delineating the protective versus pathogenic pathways triggered by macrophage-derived RELMα could provide therapeutic insight into tipping the balance towards host protective immunity against hookworms.

ACKNOWLEDGEMENTS

ABBREVIATIONS:

AAMac	Alternatively activated macrophages
AMICA1	Adhesion molecule, interacting with CXADR antigen 1
ARG1	Arginase I
ATP	Adenosine triphosphate
BAL	Bronchoalveolar lavage
BCL2	B-cell lymphoma 2
BM	Bone marrow
CCL3	Chemokine (C-C motif) ligand 3
CCL6	Chemokine (C-C motif) ligand 6
CCL19	Chemokine (C-C motif) ligand 19
CHIL3	Chitinase-like 3
DEG	Differentially expressed genes
EC	Epithelial cell
ELISA	Enzyme-linked immunosorbent assay
FACS	Florescent activated cell sorting
FBS	Fetal bovine serum
FCNB	Ficolin B
FGF18	Fibroblast growth factor 18
FPR-RS5	N-formylpeptide receptor
GAPDH	Glyceraldehyde 3-phosphate dehydrogenase
GSL	*Griffonia simplicifolia* lectin
H&E	Hematoxylin and eosin
IF	Immunofluorescence
JAM	Junctional adhesion molecule
L3	Infectious third-stage larvae
MIF	Macrophage migration inhibitory factor
MMP19	Matrix metallopeptidase 19
Nb	Nippostronglylus brasiliensis

PS	Pathway score
PBS	Phosphate buffered saline
PDGFRA	Platelet-derived growth factor receptor alpha
PFA	Paraformaldehyde
RELM	Resistin-Like Molecule
RGS1	Regulator of G-protein signaling
RT-PCR	Real time polymerase chain reaction
SEM	Scanning electron microscopy
Th1	T helper type 1
Th2	T helper type 2
TM7SF3	Transmembrane 7 superfamily member
TREM2	Triggering receptor expressed on myeloid cells 2
WT	Wild-type

REFERENCES

1. Urban JF, Katona IM, Paul WE, Finkelman FD (1991) Interleukin 4 is important in protective immunity to a gastrointestinal nematode infection in mice. Proc Natl Acad Sci U S A 88, 5513–7. [PubMed: 2062833]

2. Finkelman FD, Shea-Donohue T, Morris SC, Gildea L, Strait R, Madden KB, Schopf L, Urban JF (2004) Interleukin-4- and interleukin-13-mediated host protection against intestinal nematode parasites. Immunol Rev 201, 139–55. [PubMed: 15361238]

3. Grencis RK (2015) Immunity to helminths: resistance, regulation, and susceptibility to gastrointestinal nematodes. Annu Rev Immunol 33, 201–25. [PubMed: 25533702]

4. Nono JK, Ndlovu H, Abdel Aziz N, Mpotje T, Hlaka L, Brombacher F (2017) Interleukin-4 receptor alpha is still required after Th2 polarization for the maintenance and the recall of protective immunity to Nematode infection. PLoS Negl Trop Dis 11, e0005675. [PubMed: 28651009]

5. Chen F, Liu Z, Wu W, Rozo C, Bowdridge S, Millman A, Van Rooijen N, Urban JF, Wynn TA, Gause WC (2012) An essential role for TH2-type responses in limiting acute tissue damage during experimental helminth infection. Nat Med 18, 260–6. [PubMed: 22245779]

6. Gause WC, Wynn TA, Allen JE (2013) Type 2 immunity and wound healing: evolutionary refinement of adaptive immunity by helminths. Nat Rev Immunol 13, 607–14. [PubMed: 23827958]

7. Novak ML and Koh TJ (2013) Macrophage phenotypes during tissue repair. J Leukoc Biol 93, 875–81. [PubMed: 23505314]

8. Chiaramonte MG, Cheever AW, Malley JD, Donaldson DD, Wynn TA (2001) Studies of murine schistosomiasis reveal interleukin-13 blockade as a treatment for established and progressive liver fibrosis. Hepatology 34, 273–82. [PubMed: 11481612]

9. Fallon PG, Emson CL, Smith P, McKenzie AN (2001) IL-13 overexpression predisposes to anaphylaxis following antigen sensitization. J Immunol 166, 2712–6. [PubMed: 11160336]

10. Gause WC, and Artis David, eds. (2015) T*he Th2 Type Immune Response in Health and Disease: From Host Defense and Allergy to Metabolic Homeostasis and Beyond.* Springer.

11. Holcomb IN, Kabakoff RC, Chan B, Baker TW, Gurney A, Henzel W, Nelson C, Lowman HB, Wright BD, Skelton NJ, Frantz GD, Tumas DB, Peale FV, Shelton DL, Hebert CC (2000) FIZZ1,

a novel cysteine-rich secreted protein associated with pulmonary inflammation, defines a new gene family. EMBO J 19, 4046–55. [PubMed: 10921885]

12. Steppan CM, Brown EJ, Wright CM, Bhat S, Banerjee RR, Dai CY, Enders GH, Silberg DG, Wen X, Wu GD, Lazar MA (2001) A family of tissue-specific resistin-like molecules. Proc Natl Acad Sci U S A 98, 502–6. [PubMed: 11209052]

13. Nair MG, Du Y, Perrigoue JG, Zaph C, Taylor JJ, Goldschmidt M, Swain GP, Yancopoulos GD, Valenzuela DM, Murphy A, Karow M, Stevens S, Pearce EJ, Artis D (2009) Alternatively activated macrophage-derived RELM-{alpha} is a negative regulator of type 2 inflammation in the lung. J Exp Med 206, 937–52. [PubMed: 19349464]

14. Munitz A, Waddell A, Seidu L, Cole ET, Ahrens R, Hogan SP, Rothenberg ME (2008) Resistin-like molecule alpha enhances myeloid cell activation and promotes colitis. J Allergy Clin Immunol 122, 1200–1207.e1. [PubMed: 19084112]

15. Munitz A, Seidu L, Cole ET, Ahrens R, Hogan SP, Rothenberg ME (2009) Resistin-like molecule alpha decreases glucose tolerance during intestinal inflammation. J Immunol 182, 2357–63. [PubMed: 19201890]

16. Bokarewa M, Nagaev I, Dahlberg L, Smith U, Tarkowski A (2005) Resistin, an adipokine with potent proinflammatory properties. J Immunol 174, 5789–95. [PubMed: 15843582]

17. Munitz A, Cole ET, Karo-Atar D, Finkelman FD, Rothenberg ME (2012) Resistin-like molecule-α regulates IL-13-induced chemokine production but not allergen-induced airway responses. Am J Respir Cell Mol Biol 46, 703–13. [PubMed: 22246861]

18. Dong L, Wang SJ, Camoretti-Mercado B, Li HJ, Chen M, Bi WX (2008) FIZZ1 plays a crucial role in early stage airway remodeling of OVA-induced asthma. J Asthma 45, 648–53. [PubMed: 18951255]

19. Chen G, Wang SH, Jang JC, Odegaard JI, Nair MG (2016) Comparison of RELMα and RELMβ Single- and Double-Gene-Deficient Mice Reveals that RELMα Expression Dictates Inflammation and Worm Expulsion in Hookworm Infection. Infect Immun 84, 1100–11. [PubMed: 26831469]

20. Lee MR, Shim D, Yoon J, Jang HS, Oh SW, Suh SH, Choi JH, Oh GT (2014) Retnla overexpression attenuates allergic inflammation of the airway. PLoS One 9, e1

21. Pesce JT, Ramalingam TR, Wilson MS, Mentink-Kane MM, Thompson RW, Cheever AW, Urban JF, Wynn TA (2009) Retnla (relmalpha/fizz1) suppresses helminth-induced Th2-type immunity. PLoS Pathog 5, e1000393. [PubMed: 19381262]

22. Siracusa MC, Reece JJ, Urban JF, Scott AL (2008) Dynamics of lung macrophage activation in response to helminth infection. J Leukoc Biol 84, 1422–33. [PubMed: 18719016]

23. Cook PC, Jones LH, Jenkins SJ, Wynn TA, Allen JE, MacDonald AS (2012) Alternatively activated dendritic cells regulate CD4+ T-cell polarization in vitro and in vivo. Proc Natl Acad Sci U S A 109, 9977–82. [PubMed: 22660926]

24. Raes G, De Baetselier P, Noël W, Beschin A, Brombacher F, Hassanzadeh Gh G (2002) Differential expression of FIZZ1 and Ym1 in alternatively versus classically activated macrophages. J Leukoc Biol 71, 597–602. [PubMed: 11927645]

25. Wills-Karp M, Rani R, Dienger K, Lewkowich I, Fox JG, Perkins C, Lewis L, Finkelman FD, Smith DE, Bryce PJ, Kurt-Jones EA, Wang TC, Sivaprasad U, Hershey GK, Herbert DR (2012) Trefoil factor 2 rapidly induces interleukin 33 to promote type 2 immunity during allergic asthma and hookworm infection. J Exp Med 209, 607–22. [PubMed: 22329990]

26. Esser-von Bieren J, Mosconi I, Guiet R, Piersgilli A, Volpe B, Chen F, Gause W, Seitz A, Verbeek JS, Harris NL (2013) Antibodies trap tissue migrating helminth larvae and prevent tissue damage by driving IL-4Rα-independent alternative differentiation of macrophages. PLoS Pathog 9, e1003771. [PubMed: 24244174]

27. Tomfohr J, Lu J, Kepler TB Pathway level analysis of gene expression using singular value decomposition. BMC Bioinformatics.

28. Nair MG, Gallagher IJ, Taylor MD, Loke P, Coulson PS, Wilson RA, Maizels RM, Allen JE (2005) Chitinase and Fizz family members are a generalized feature of nematode infection with selective upregulation of Ym1 and Fizz1 by antigen-presenting cells. Infect Immun 73, 385–94. [PubMed: 15618176]

29. Chen F, Wu W, Millman A, Craft JF, Chen E, Patel N, Boucher JL, Urban JF, Kim CC, Gause WC (2014) Neutrophils prime a long-lived effector macrophage phenotype that mediates accelerated helminth expulsion. Nat Immunol 15, 938–46. [PubMed: 25173346]

30. Su Q, Zhou Y, Johns RA (2007) Bruton's tyrosine kinase (BTK) is a binding partner for hypoxia induced mitogenic factor (HIMF/FIZZ1) and mediates myeloid cell chemotaxis. FASEB J 21, 1376–82. [PubMed: 17264170]

31. Li D, Fernandez LG, Dodd-o J, Langer J, Wang D, Laubach VE (2005) Upregulation of hypoxia-induced mitogenic factor in compensatory lung growth after pneumonectomy. Am J Respir Cell Mol Biol 32, 185–91. [PubMed: 15626779]

32. Teng X, Li D, Champion HC, Johns RA (2003) FIZZ1/RELMα, a Novel Hypoxia-Induced Mitogenic Factor in Lung With Vasoconstrictive and Angiogenic Properties. Circulation Research 92, 1065. [PubMed: 12714564]

33. Gao JL, Chen H, Filie JD, Kozak CA, Murphy PM (1998) Differential expansion of the N-formylpeptide receptor gene cluster in human and mouse. Genomics 51, 270–6. [PubMed: 9722950]

34. Turnbull IR, Gilfillan S, Celia M, Aoshi T, Miller M, Piccio L, Hernandez M, Colonna M (2006) Cutting edge: TREM-2 attenuates macrophage activation. J Immunol 177, 3520–4. [PubMed: 16951310]

35. Harvie M, Camberis M, Tang SC, Delahunt B, Paul W, Le Gros G (2010) The lung is an important site for priming CD4 T-cell-mediated protective immunity against gastrointestinal helminth parasites. Infect Immun 78, 3753–62. [PubMed: 20605978]

36. Thawer SG, Horsnell WG, Darby M, Hoving JC, Dewals B, Cutler AJ, Lang, Brombacher F (2014) Lung-resident CD4+ T cells are sufficient for IL-4Rα-dependent recall immunity to Nippostrongylus brasiliensis infection. Mucosal Immunol 7, 239–48. [PubMed: 23778354]

37. Horsnell WG, Darby MG, Hoving JC, Nieuwenhuizen N, McSorley HJ, Ndlovu H, Bobat S, Kimberg M, Kirstein F, Cutler AJ, Dewals B, Cunningham AF, Brombacher F (2013) IL-4Rα-associated antigen processing by B cells promotes immunity in Nippostrongylus brasiliensis infection. PLoS Pathog 9, e1003662. [PubMed: 24204255]

38. Nair MG and Herbert DR (2016) Immune polarization by hookworms: taking cues from T helper type 2, type 2 innate lymphoid cells and alternatively activated macrophages. Immunology 148, 115–24. [PubMed: 26928141]

39. Borthwick LA, Barron L, Hart KM, Vannella KM, Thompson RW, Oland S, Cheever A, Sciurba J, Ramalingam TR, Fisher AJ, Wynn TA (2016) Macrophages are critical to the maintenance of IL-13-dependent lung inflammation and fibrosis. Mucosal Immunol 9, 38–55. [PubMed: 25921340]

40. Zhao A, Urban JF, Anthony RM, Sun R, Stiltz J, van Rooijen N, Wynn TA, Gause WC, Shea-Donohue T (2008) Th2 cytokine-induced alterations in intestinal smooth muscle function depend on alternatively activated macrophages. Gastroenterology 135, 217–225.e1. [PubMed: 18471439]

41. Loke P, Nair MG, Parkinson J, Guiliano D, Blaxter M, Allen JE (2002) IL-4 dependent alternatively-activated macrophages have a distinctive in vivo gene expression phenotype. BMC Immunol 3, 7. [PubMed: 12098359]

42. Artis D, Wang ML, Keilbaugh SA, He W, Brenes M, Swain GP, Knight PA, Donaldson DD, Lazar MA, Miller HR, Schad GA, Scott P, Wu GD (2004) RELMbeta/FIZZ2 is a goblet cell-specific immune-effector molecule in the gastrointestinal tract. Proc Natl Acad Sci U S A 101, 13596–600. [PubMed: 15340149]

43. Herbert DR, Yang JQ, Hogan SP, Groschwitz K, Khodoun M, Munitz A, Orekov T, Perkins C, Wang Q, Brombacher F, Urban JF, Rothenberg ME, Finkelman FD (2009) Intestinal epithelial cell secretion of RELM-beta protects against gastrointestinal worm infection. J Exp Med 206, 2947–57. [PubMed: 19995957]

44. Le Y, Murphy PM, Wang JM (2002) Formyl-peptide receptors revisited. Trends Immunol 23, 541–8. [PubMed: 12401407]

45. Endo Y, Iwaki D, Ishida Y, Takahashi M, Matsushita M, Fujita T (2012) Mouse ficolin B has an ability to form complexes with mannose-binding lectin-associated serine proteases and activate complement through the lectin pathway. J Biomed Biotechnol 2012, 105891. [PubMed: 22523468]

46. Bonne-Année S, Kerepesi LA, Hess JA, O'Connell AE, Lok JB, Nolan TJ, Abraham D (2013) Human and mouse macrophages collaborate with neutrophils to kill larval Strongyloides stercoralis. Infect Immun 81, 3346–55. [PubMed: 23798541]

47. Guo YL, Bai R, Chen CX, Liu DQ, Liu Y, Zhang CY, Zen K (2009) Role of junctional adhesion molecule-like protein in mediating monocyte transendothelial migration. Arterioscler Thromb Vase Biol 29, 75–83.

48. Wei W, Mok SC, Oliva E, Kim SH, Mohapatra G, Birrer MJ (2013) FGF18 as a prognostic and therapeutic biomarker in ovarian cancer. J Clin Invest 123, 4435–48. [PubMed: 24018557]

49. Knipper JA, Willenborg S, Brinckmann J, Bloch W, MaaB T, Wagener R, Krieg T, Sutherland T, Munitz A, Rothenberg ME, Niehoff A, Richardson R, Hammerschmidt M, Allen JE, Eming SA (2015) Interleukin-4 Receptor α Signaling in Myeloid Cells Controls Collagen Fibril Assembly in Skin Repair. Immunity 43, 803–16. [PubMed: 26474656]

50. Caley MP, Martins VL, O'Toole EA (2015) Metalloproteinases and Wound Healing. Adv Wound Care (New Rochelle) 4, 225–234. [PubMed: 25945285]

51. Liu T, Yu H, Ullenbruch M, Jin H, Ito T, Wu Z, Liu J, Phan SH (2014) The in vivo fibrotic role of FIZZ1 in pulmonary fibrosis. PLoS One 9, e88362. [PubMed: 24516640]

52. Horikawa S, Ishii Y, Hamashima T, Yamamoto S, Mori H, Fujimori T, Shen J, Inoue R, Nishizono H, Itoh H, Majima M, Abraham D, Miyawaki T, Sasahara M (2015) PDGFRα plays a crucial role in connective tissue remodeling. Sci Rep 5, 17948. [PubMed: 26639755]

53. Isaac R, Goldstein T, Furth N, Zilber N, Streim S, Boura-Halfon S, Elhanany E, Rotter V, Oren M, Zick Y (2017) TM7SF3, a novel p53-regulated homeostatic factor, attenuates cellular stress and the subsequent induction of the unfolded protein response. Cell Death Differ 24, 132–143. [PubMed: 27740623]

54. Rouault JP, Falette N, Guéhenneux F, Guillot C, Rimokh R, Wang Q, Berthet C, Moyret-Lalle C, Savatier P, Pain B, Shaw P, Berger R, Samarut J, Magaud JP, Ozturk M, Samarut C, Puisieux A (1996) Identification of BTG2, an antiproliferative p53-dependent component of the DNA damage cellular response pathway. Nat Genet 14, 482–6. [PubMed: 8944033]

55. Yamaji-Kegan K, Takimoto E, Zhang A, Weiner NC, Meuchel LW, Berger AD, Cheadle C, Johns RA (2014) Hypoxia-induced mitogenic factor (FIZZ1/RELMα) induces endothelial cell apoptosis and subsequent interleukin-4-dependent pulmonary hypertension. Am J Physiol Lung Cell Mol Physiol 306, LI090–103.

56. Tong Q, Zheng L, Li B, Wang D, Huang C, Matuschak GM, Li D (2006) Hypoxia-induced mitogenic factor enhances angiogenesis by promoting proliferation and migration of endothelial cells. Exp Cell Res 312, 3559–69. [PubMed: 16982054]

57. Patel J, McNeill E, Douglas G, Hale AB, de Bono J, Lee R, Iqbal AJ, Regan-Komito D, Stylianou E, Greaves DR, Channon KM (2015) RGS1 regulates myeloid cell accumulation in atherosclerosis and aortic aneurysm rupture through altered chemokine signalling. Nat Commun 6, 6614. [PubMed: 25782711]

58. Lamb EW, Crow ET, Lim KC, Liang YS, Lewis FA, Davies SJ (2007) Conservation of CD4+ T cell-dependent developmental mechanisms in the blood fluke pathogens of humans. Int J Parasitol 37, 405–15. [PubMed: 17196594]

59. Riner DK, Ferragine CE, Maynard SK, Davies SJ (2013) Regulation of innate responses during pre-patent schistosome infection provides an immune environment permissive for parasite development. PLoS Pathog 9, e1003708. [PubMed: 24130499]

60. Lamb EW, Walls CD, Pesce JT, Riner DK, Maynard SK, Crow ET, Wynn TA, Schaefer BC, Davies SJ (2010) Blood fluke exploitation of non-cognate CD4+ T cell help to facilitate parasite development. PLoS Pathog 6, e1000892. [PubMed: 20442785]

61. Bouchery T, Filbey K, Shepherd A, Chandler J, Patel D, Schmidt A, Camberis M, Peignier A, Smith AAT, Johnston K, Painter G, Pearson M, Giacomin P, Loukas A, Bottazzi ME, Hotez P, LeGros G (2018) A novel blood-feeding detoxification pathway in Nippostrongylus brasiliensis L3 reveals a potential checkpoint for arresting hookworm development. PLoS Pathog 14, e1006931. [PubMed: 29566094]

62. Harris NL and Loke P (2017) Recent Advances in Type-2-Cell-Mediated Immunity: Insights from Helminth Infection. Immunity 47, 1024–1036. [PubMed: 29262347]

63. Moog-Lutz C, Cavé-Riant F, Guibal FC, Breau MA, Di Gioia Y, Couraud PO, Cayre YE, Bourdoulous S, Lutz PG (2003) JAML, a novel protein with characteristics of a junctional adhesion molecule, is induced during differentiation of myeloid leukemia cells. Blood 102, 3371–8. [PubMed: 12869515]

64. Luster AD, Alon R, von Andrian UH (2005) Immune cell migration in inflammation: present and future therapeutic targets. Nat Immunol 6, 1182–90. [PubMed: 16369557]

65. Mackay CR (2008) Moving targets: cell migration inhibitors as new anti-inflammatory therapies. Nat Immunol 9, 988–98. [PubMed: 18711436]

66. Reim I, Hollfelder D, Ismat A, Frasch M (2012) The FGF8-related signals Pyramus and Thisbe promote pathfinding, substrate adhesion, and survival of migrating longitudinal gut muscle founder cells. Dev Biol 368, 28–43. [PubMed: 22609944]

67. VanCompernolle SE, Clark KL, Rummel KA, Todd SC (2003) Expression and function of formyl peptide receptors on human fibroblast cells. J Immunol 171, 2050–6. [PubMed: 12902510]

68. Sadanandam A, Rosenbaugh EG, Singh S, Varney M, Singh RK (2010) Semaphorin 5A promotes angiogenesis by increasing endothelial cell proliferation, migration, and decreasing apoptosis. Microvasc Res 79, 1–9. [PubMed: 19850054]

69. Endo Y, Takahashi M, Iwaki D, Ishida Y, Nakazawa N, Kodama T, Matsuzaka T, Kanno K, Liu Y, Tsuchiya K, Kawamura T, Ikawa M, Waguri S, Wada I, Matsushita M, Schwaeble WJ, Fujita T (2012) Mice deficient in ficolin, a lectin complement pathway recognition molecule, are susceptible to Streptococcus pneumoniae infection. J Immunol 189, 5860–6. [PubMed: 23150716]

70. Sibilano R, Gaudenzio N, DeGorter MK, Reber LL, Hernandez JD, Starkl PM, Zurek OW, Tsai M, Zahner S, Montgomery SB, Roers A, Kronenberg M, Yu M, Galli SJ (2016) A TNFRSF14-FcεRI-mast cell pathway contributes to development of multiple features of asthma pathology in mice. Nat Commun 7, 13696. [PubMed: 27982078]

71. Lu P, Takai K, Weaver VM, Werb Z (2011) Extracellular matrix degradation and remodeling in development and disease. Cold Spring Harb Perspect Biol 3.

72. Szerlip NJ, Pedraza A, Chakravarty D, Azim M, McGuire J, Fang Y, Ozawa T, Holland EC, Huse JT, Jhanwar S, Leversha MA, Mikkelsen T, Brennan CW (2012) Intratumoral heterogeneity of receptor tyrosine kinases EGFR and PDGFRA amplification in glioblastoma defines subpopulations with distinct growth factor response. Proc Natl Acad Sci U S A 109, 3041–6. [PubMed: 22323597]

73. Kornfeld JW, Baitzel C, Könner AC, Nicholls HT, Vogt MC, Herrmanns K, Scheja L, Haumaitre C, Wolf AM, Knippschild U, Seibler J, Cereghini S, Heeren J, Stoffel M, Brüning JC (2013) Obesity-induced overexpression of miR-802 impairs glucose metabolism through silencing of Hnf1b. Nature 494, 111–5. [PubMed: 23389544]

74. Attery A and Batra JK (2017) Mouse eosinophil associated ribonucleases: Mechanism of cytotoxic, antibacterial and antiparasitic activities. Int J Biol Macromol 94, 445–450. [PubMed: 27765572]
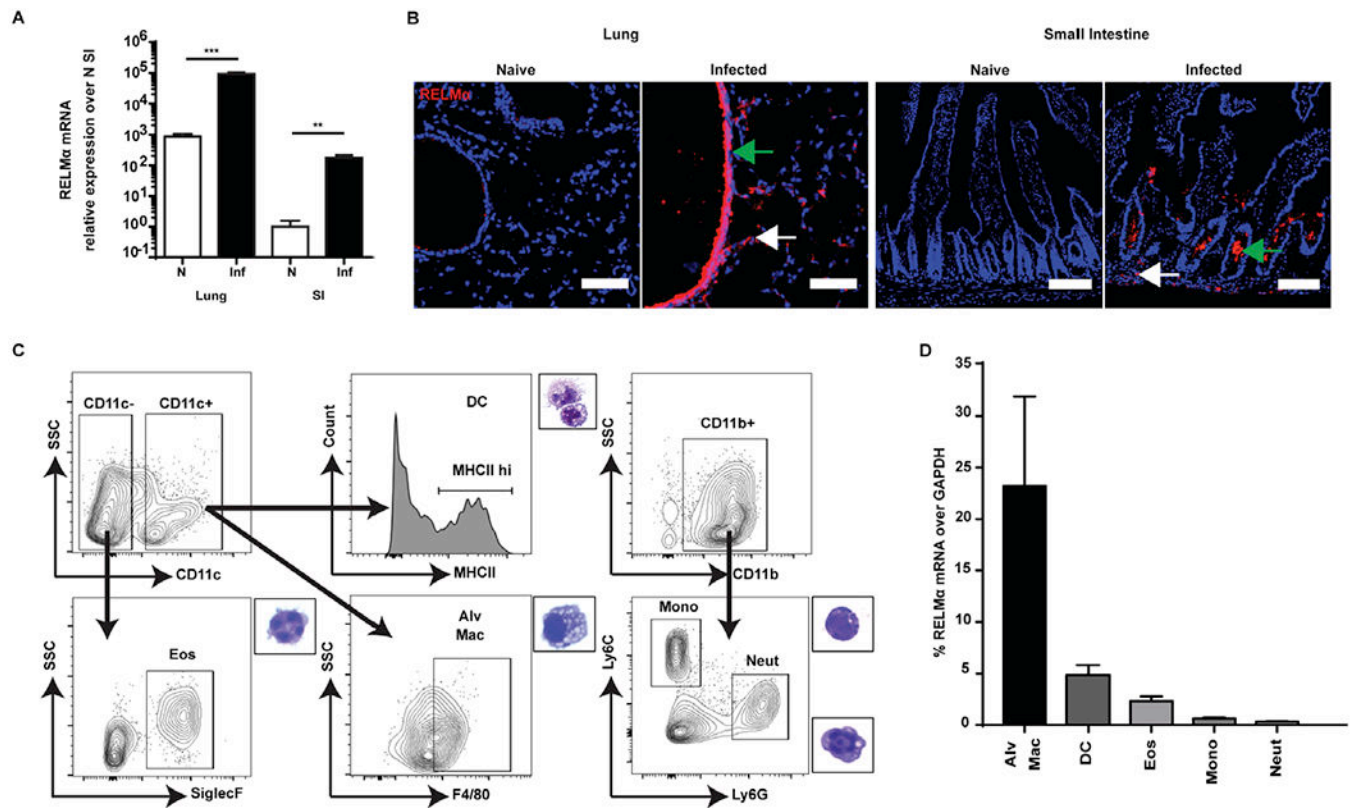
Figure 1: *Nb* **infection induces RELMα expression in ECs and alveolar macrophages.**
C57BL/6 mice were left naïve or infected with *Nb* and evaluated for RELMα expression at day 7 post-infection. (A) RELMα RT-PCR in lung and small intestine (SI) was measured as relative fold induction over naïve SI (n=3 mice per group). (B) IF staining of RELMα (red) and DAPI (blue) was performed in naïve and day 7 *Nb*-infected tissue. Lung; green arrow indicates airway cells and white arrow indicates parenchymal cells. SI; green arrow indicates basal crypts and white arrow indicates circulating leukocytes (scale bar, 100 μm). (C) Gating strategy and confirmatory H&E cytospin for FACS sorted lung cells from *Nb*-infected mice. (D) RELMα mRNA expression was quantified in sorted alveolar macrophages (Alv Mac), dendritic cells (DC), eosinophils (Eos), monocytes (Mono) and neutrophils (Neut) as fold induction over neutrophils (n=4-6 mice per group). Data are represented as mean ± SEM.
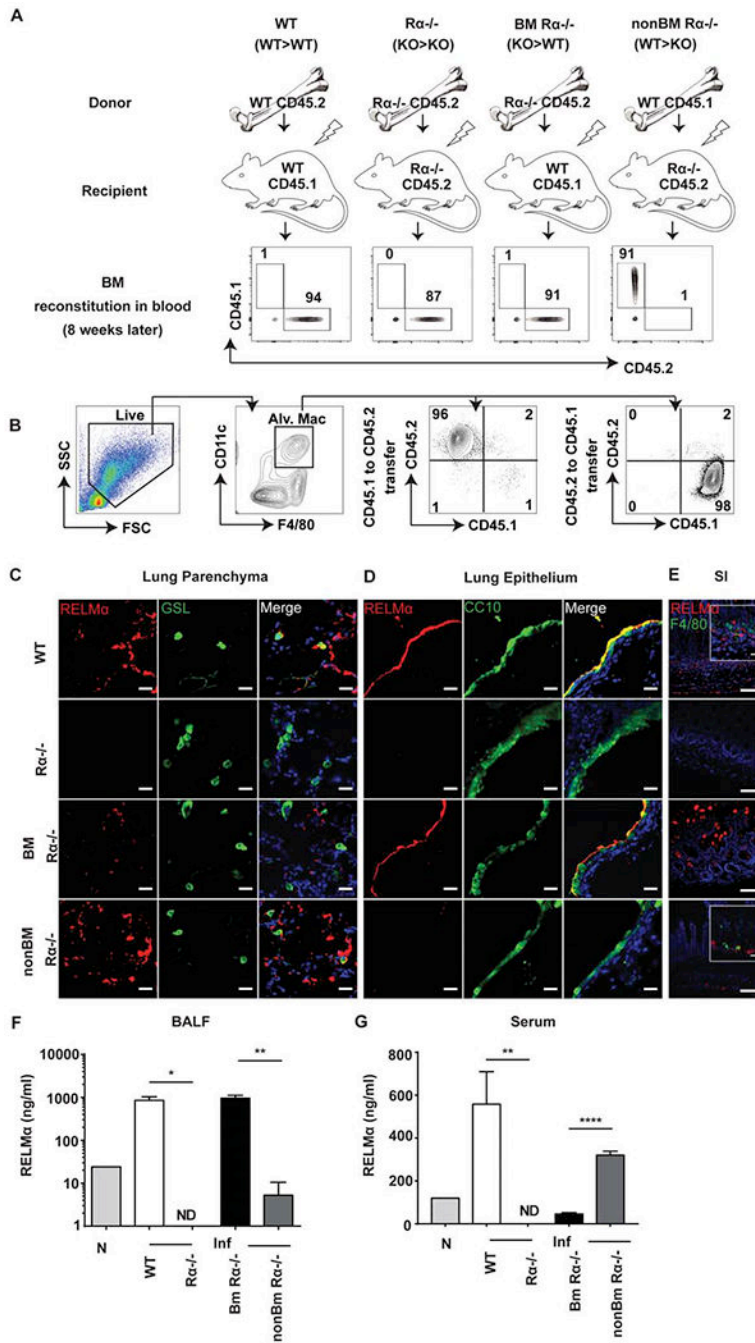
Figure 2: Generation of RELMα^{−/−} BM chimeras to determine the contribution of BM and non BM-derived RELMα in *Nb* infection.

(A) BM chimera design and validation by flow cytometric analysis of peripheral blood. (B) Evaluation of alveolar macrophage reconstitution in bone marrow chimeric mice. (C-E) Day 9 *Nb*-infected BM chimeras were evaluated for RELMα expression by IF staining followed by microscopic examination. (C) Lung parenchyma and (D) lung epithelium stained for RELMα (red), GSL/CC10 (green) and DAPI (blue) (scale bar, 25 μm). (E) Small intestine stained for RELMα (red), F4/80 (green) and DAPI (blue) (scale bar, 200 μm, insert 50 μm). (F-G) RELMα levels in the BAL fluid (F) and serum (G) of day 9 *Nb*-infected BM chimeras

were measured by ELISA (ND not detected, n=4 mice per group). Data are presented as mean ± SEM, and representative of 3 separate experiments.
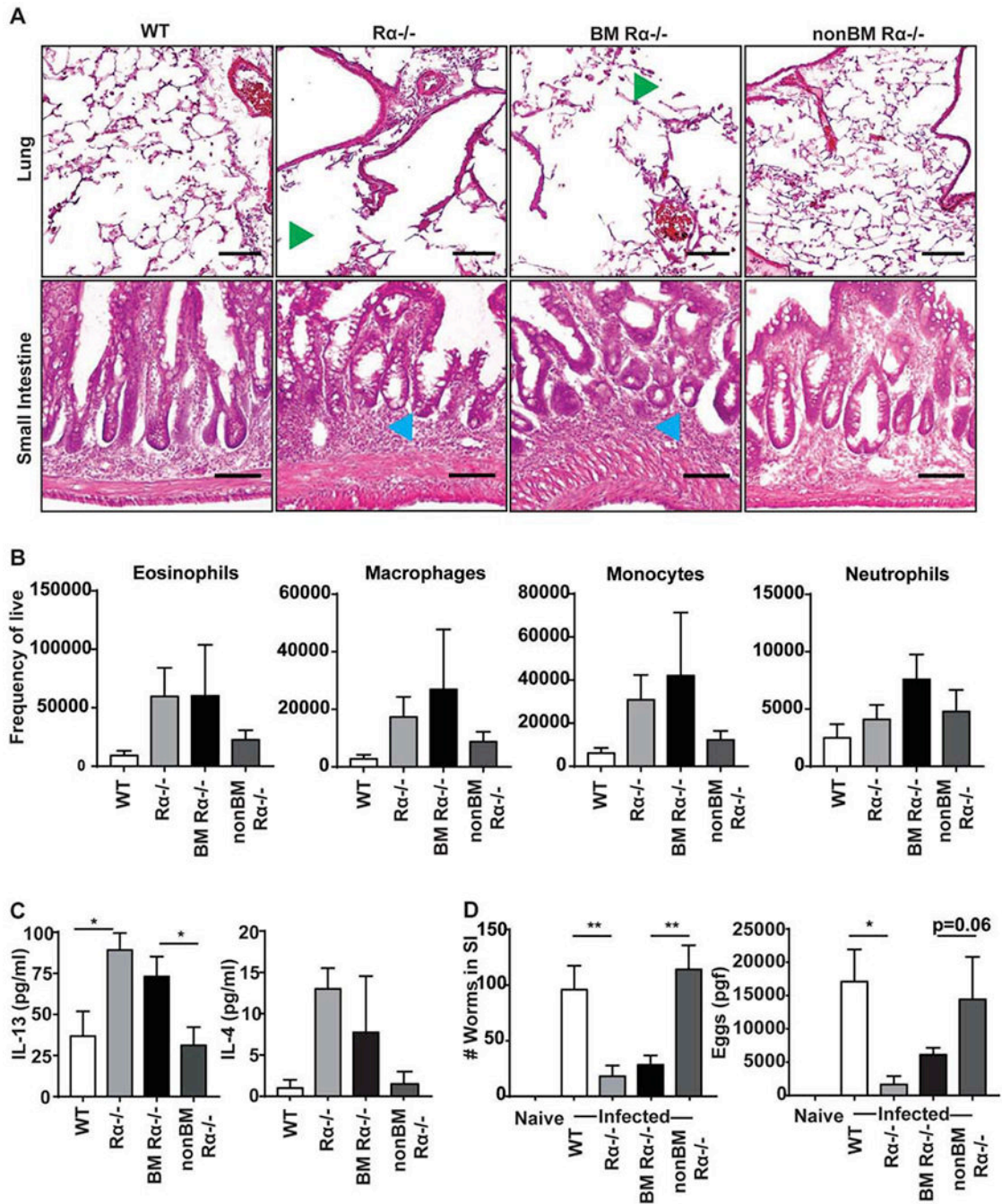
Figure 3: BM-derived RELMα regulates *Nb* infection-induced tissue inflammation, Th2 immune responses and parasite expulsion.

BM chimeras were infected with *Nb* and sacrificed at day 9 to evaluate *Nb* immune responses and burdens. (A) H&E stained sections of *Nb*-infected lung and SI tissue (Green arrow, airway destruction; Blue arrow, infiltrating leukocytes; scale bar, 200 μm). (B) Flow cytometric analysis of BAL cell populations in infected mice (n=3-4 mice per group. (C) IL-13 and IL-4 protein levels were measured by ELISA in serum and BAL fluid respectively of infected mice (n=3-6 mice per group). (D) Intestinal worm and fecal egg burdens were measured at day 9 post-infection (n=8-21 mice per group). For panel D egg burden, log

transformation of the raw data was done prior to statistical analysis. Data are presented as mean ± SEM.

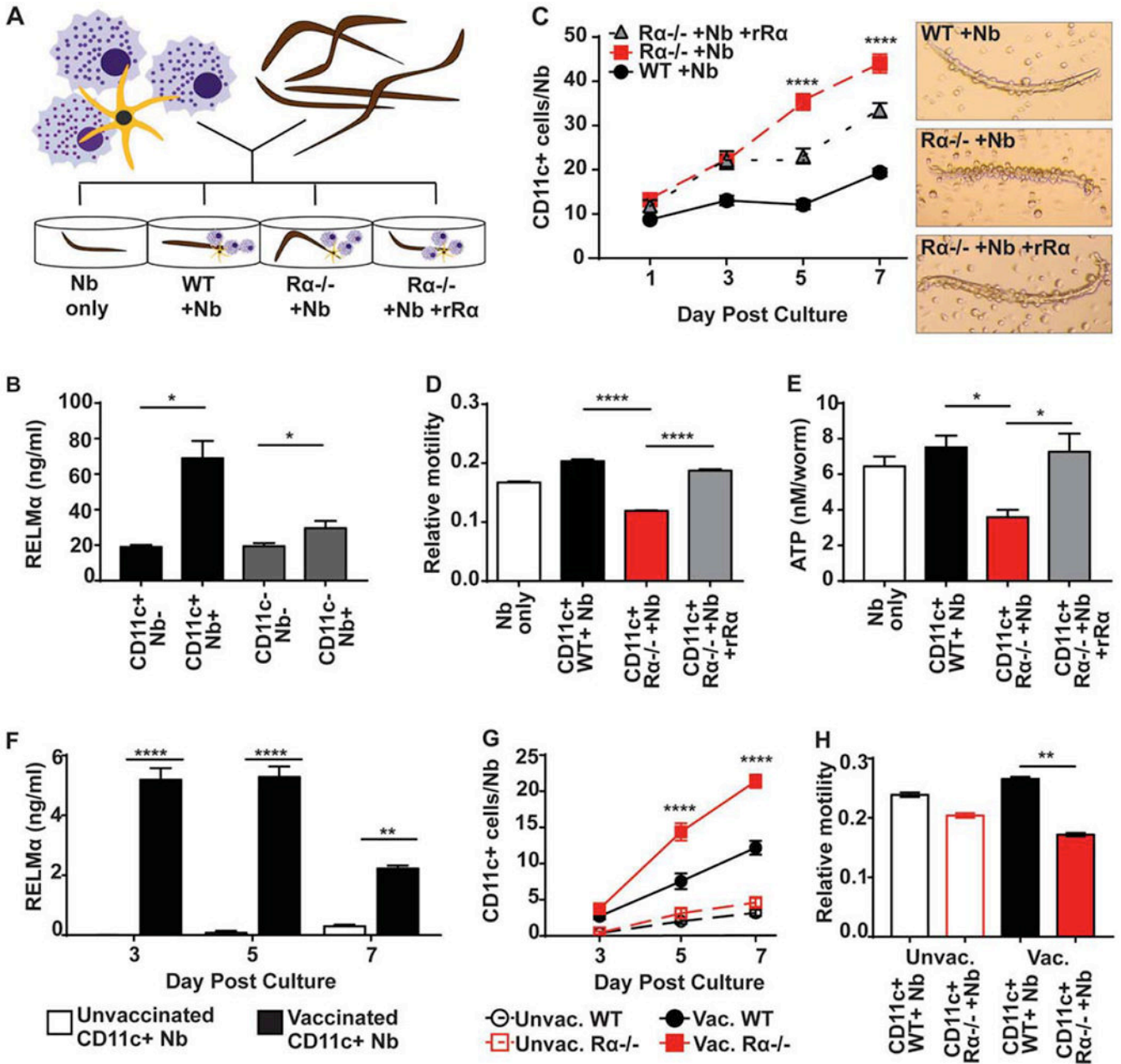**Figure 4: RELMα⁻/⁻ CD11c⁺ lung macrophages have enhanced ability to bind and impair *Nb* fitness.**

(A) Design of co-culture assay of *Nb* L3 with lung cells from day 21 *Nb*-infected WT or RELMα⁻/⁻ mice. (B) RELMα secretion by WT cells was measured in supernatants from day 3 post culture of CD11c positive and negative fractions from lung cells with or without *Nb*. (C) Microscopic quantification of adherent cells to *Nb* was performed for co-culture with CD11c⁺ cells from WT or RELMα⁻/⁻ mice and representative bright field images shown. (D) Relative *Nb* motility (E) and ATP levels were measured at day 7 post co-culture. Where indicated, 100 ng/ml recombinant RELMα (rRα) was added to RELMα⁻/⁻ CD11c⁺ cell-*Nb* co-culture. (F) RELMα secretion by unvaccinated *vs.* vaccinated CD11c⁺ cells were

measured at D3, 5 and 7 post-culture (n=3 per group). (G) Microscopic quantification of adherent cells to *Nb* was performed for co-culture with CD11c$^+$ cells from unvaccinated *vs.* vaccinated mice and representative bright field images are shown. (H) Relative *Nb* motility was measured at day 7 post co-culture. Data are presented as mean ± SEM (n=3/group), and representative of 2 separate experiments.
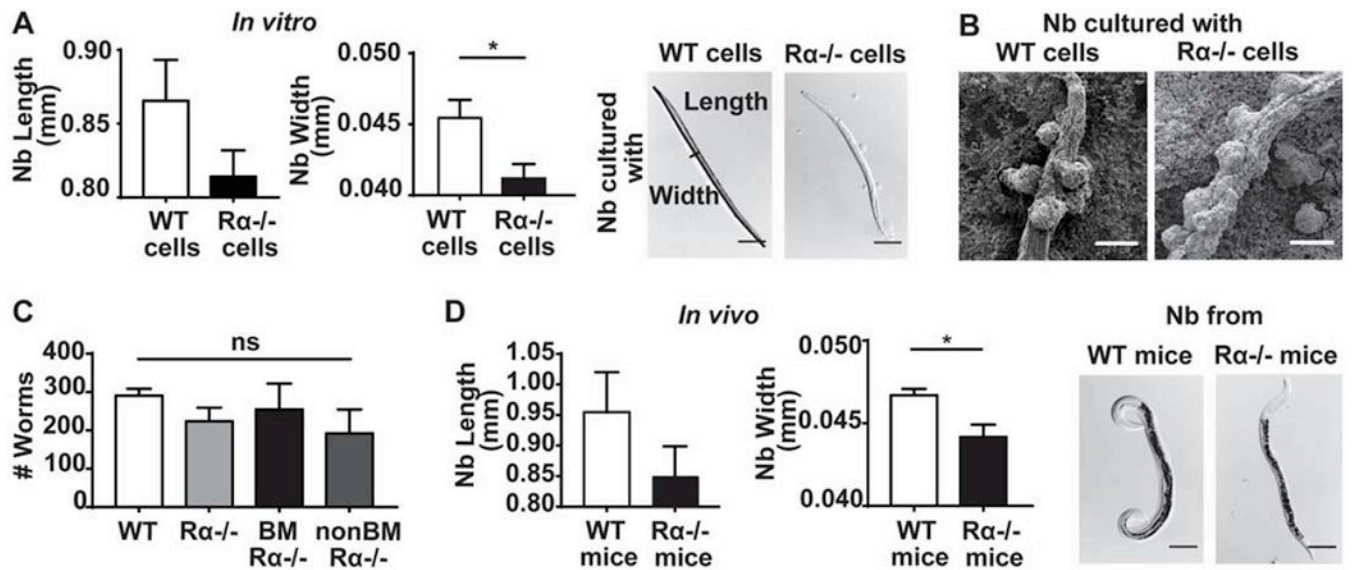
Figure 5. RELMα^{−/−} lung cells impair *Nb* growth.
Nb from day 7 co-culture assay or day 3 infected lungs of WT and RELMα−/− mice were compared. (A-B) *Nb* L3 worms from day 7 co-culture with total lung cells were measured and visualized for length and width (scale bar, 0.1 mm; n=9-11 worms per group). (B) Scanning Electron Micrograph of *Nb* L3 and CD11c+ lung macrophages at end of co-culture (scale bar, 20 μm). (C) *Nb* larvae were collected from day 3 A7>-infected WT or RELMα−/− mice, counted, and (D) measured and visualized for length and width (scale bar, 0.1 mm; n=5-6 worms per group). Data are presented as mean ± SEM.
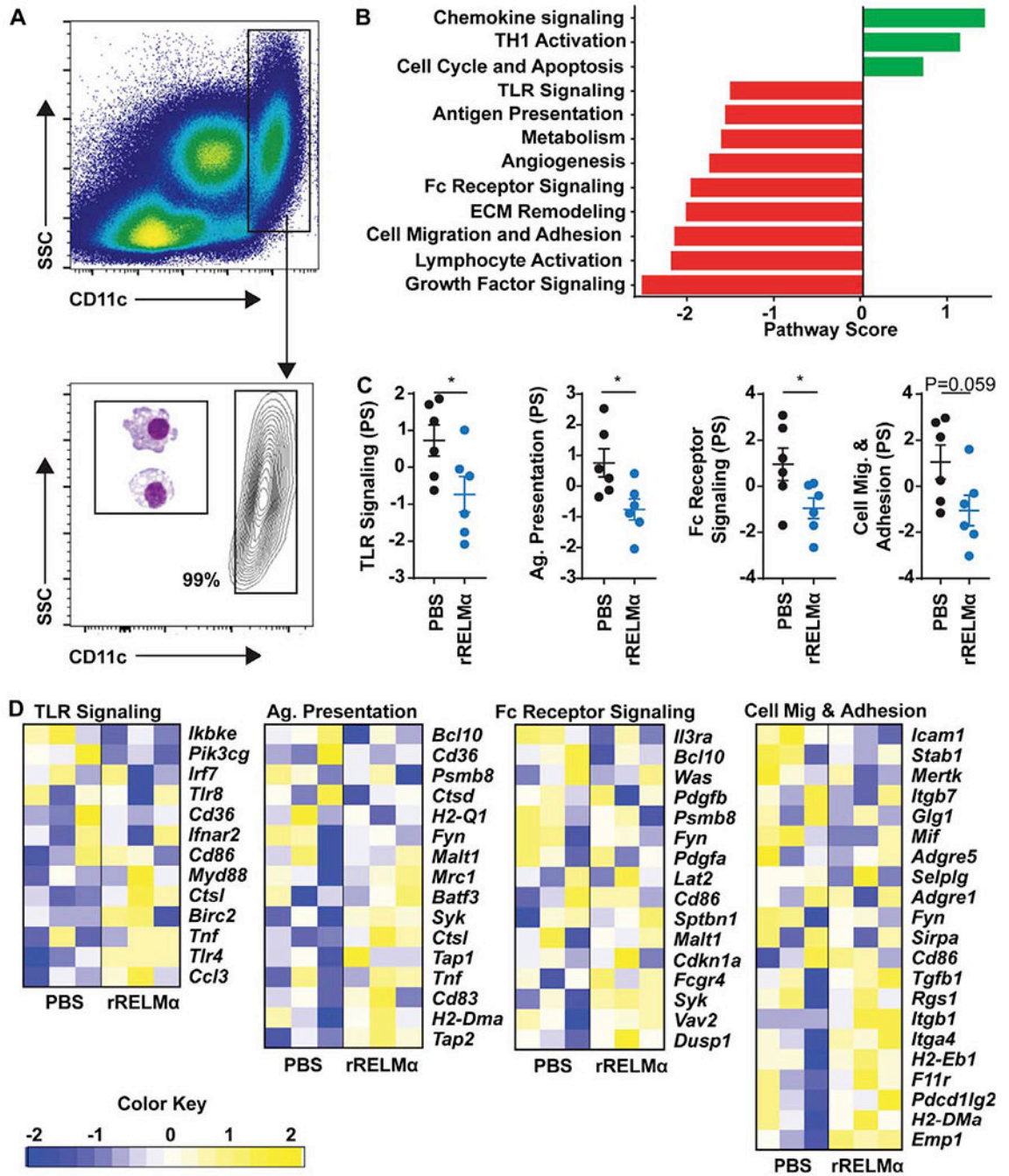
Figure 6. RELMα downregulates antigen presentation, Fc receptor signaling, TLR signaling, cell migration and adhesion.

(A) CD11c$^+$ macrophages were sorted from D9 *Nb*-infected RELMα$^{-/-}$ mouse lungs and evaluated for purity. Representative flow cytometry plot and cytospin is presented. (B) Nanostring analysis of biological pathways that were changed by RELMα (n=6 per group). (C) Biological pathways downregulated by RELMα (n=6 per group). (D) Heatmap showing individual gene expression of genes belonging to respective biological pathway (n=3 per group).

Table 1.

Differentially expressed genes in PBS *vs.* RELMα treatment.

Putative Function	RELMα suppressed	RELMα induced
Cell Cycle and Apoptosis		*Btg2*⁺
Cell Migration and Adhesion	*Mif*⁺, *Amica1*[63], *Ccl19*[64], *Ccr6*[65], *Fgf18*[66], *Fpr-rs5*[67], *Sema5a*[68]	*F11r*⁺, *Itgb1*⁺, *Rgs1*⁺
Chemokine Signaling	*Ccl19*#, *Ccr6*#,	*Ccl3*⁺, *Ccl6*⁺, *Rgs1*⁺
Lectin Signaling	*Fcnb*[69]	*Irf1*#
Cytokine/IFN Signaling		*Tm7sf3*⁺, *Il1r2*#, *Irf1*⁺, *Tnfrsf14*[70]
Differentiation and Maintenance of Myeloid Cells		*Ikzf1*⁺
ECM Remodeling	*Adamts3*[71]	*F11r*⁺, *Furin*⁺, *Itgb1*⁺, *Kcnq1ot1*⁺, *Mmp19*⁺
Growth Factor Signaling		*Bcl2*⁺, *Furin*⁺, *Itgb1*⁺, *Pdgfra*[72]
Lymphocyte Activation	*Trem2*⁺	*Golim4*⁺, *Itgb1*⁺
Metabolism	*Arg1*⁺, *Sgpp1*⁺, *Hnf1b*[73]	
Pathogen Response/TLR Signaling	*Rnase2b*[74]	*Bcl2*⁺, *Chi13*⁺, *Ccl3*⁺

⁺NanoString nCounter Advanced Analysis

#KEGG Pathway.